This article was downloaded by: [University of California, San Diego]
On: 21 August 2012, At: 11:43
Publisher: Taylor & Francis
Informa Ltd Registered in England and Wales Registered Number: 1072954 Registered office: Mortimer House, 37-41 Mortimer Street, London W1T 3JH, UK

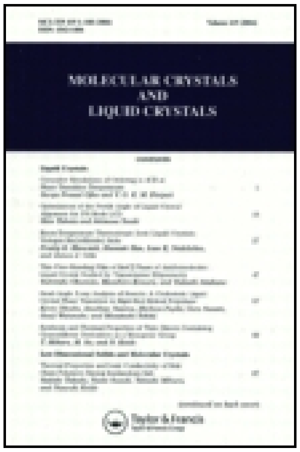

Molecular Crystals and Liquid Crystals Science and Technology. Section A. Molecular Crystals and Liquid Crystals

Publication details, including instructions for authors and subscription information:
http://www.tandfonline.com/loi/gmcl19

Anharmonic Linewidth Calculation in 1,4-Dibromobenzeneand Disordered 1,4-Bromochlorobenzene

Giorgio F. Signorini [a] , Claudia Taiti [a] & Barbara Caldarone [a]

[a] Laboratorio di Spettroscopia Molecolare, Dipartimento di Chimica, Università di Firenze, via G. Capponi 9, 50121, Firenze, Italy

Version of record first published: 04 Oct 2006

To cite this article: Giorgio F. Signorini, Claudia Taiti & Barbara Caldarone (1997): Anharmonic Linewidth Calculation in 1,4-Dibromobenzeneand Disordered 1,4-Bromochlorobenzene, Molecular Crystals and Liquid Crystals Science and Technology. Section A. Molecular Crystals and Liquid Crystals, 307:1, 189-204

To link to this article: http://dx.doi.org/10.1080/10587259708047096

PLEASE SCROLL DOWN FOR ARTICLE

Full terms and conditions of use: http://www.tandfonline.com/page/terms-and-conditions

This article may be used for research, teaching, and private study purposes. Any substantial or systematic reproduction, redistribution, reselling, loan, sub-licensing, systematic supply, or distribution in any form to anyone is expressly forbidden.

The publisher does not give any warranty express or implied or make any representation that the contents will be complete or accurate or up to date. The accuracy of any instructions, formulae, and drug doses should be independently verified with primary sources. The publisher shall not be liable for any loss, actions, claims, proceedings, demand, or costs or damages whatsoever or howsoever caused arising directly or indirectly in connection with or arising out of the use of this material.

Mol. Cryst. Liq. Cryst., 1997, Vol. 307, pp. 189–204
Reprints available directly from the publisher
Photocopying permitted by license only

© 1997 OPA (Overseas Publishers Association)
Amsterdam B.V. Published under license
in The Netherlands under the Gordon and Breach
Science Publishers imprint
Printed in India

Downloaded by [University of California, San Diego] at 11:43 21 August 2012

Anharmonic Linewidth Calculation in 1,4-Dibromobenzene and Disordered 1,4-Bromochlorobenzene

GIORGIO F. SIGNORINI*, CLAUDIA TAITI
and BARBARA CALDARONE

*Laboratorio di Spettroscopia Molecolare, Dipartimento di Chimica,
Università di Firenze, via G. Capponi 9, 50121 Firenze, Italy*

(Received 23 December 1996; In final form 20 February 1997)

As a natural extension of a preceding work on the vibrational linewidths in two isomorphic 1,4-dihalobenzenes crystals (DBB and BCB, which is orientationally disordered), calculations of the anharmonic contribution to the linewidths have been performed. The calculations show that the decay mechanisms that were previously postulated are compatible with the intermolecular potential. Some corrections to previous results are illustrated. The disorder contribution to the linewidth and its dependence on the relaxing mode are briefly discussed.

Keywords: Anharmonic linewidth calculation; vibrational relaxation; orientational disorder; 1,4-dibromobenzene; 1,4-bromochlorobenzene

1. INTRODUCTION

It is known that structural disorder has a broadening effect on vibrational bands of molecular crystals. Experimental evidence has been reviewed recently [1]. The general theory for this subject, in a perturbative framework, is well established [2, 3].

Currently, two topics appear to be of major interest: the concurrent effect of disorder and anharmonicity on line broadening; and the dependence of disorder linewidth on the relevant disorder parameter (e.g., impurity concentration) and on the type of vibrational band.

---

*Author to whom correspondence should be addressed.

Downloaded by [University of California, San Diego] at 11:43 21 August 2012

One particular kind of structural disorder is orientational disorder. Crystals of 1,4-dihalobenzenes are well suited for the investigation of the effect of static orientational disorder on vibrational bandwidths. 1,4-bromochlorobenzene (BCB) has been reported to be orientationally disordered with respect to the interchange of the two halogens [4–6]. If the homogeneous width of its vibrational bands is compared to that of the corresponding bands in 1,4-dibromobenzene (DBB), which has the same crystal structure and very similar dynamical properties, one can isolate the contribution of disorder [7].

In a previous paper [8] Raman spectra of BCB and DBB have been reported and discussed. It has been shown there that

(1) all lattice bands have a lorentzian shape;
(2) the temperature dependence of the bandwidth Γ can be reproduced with a term due to anharmonicity plus a constant term due to disorder;
(3) the relationship between the disorder term and the kind of motion involved in the vibration can be explained qualitatively.

In that work, which was based on a perturbative model formerly illustrated and applied to the same crystals [7], the anharmonic term was reproduced with an average third-order and a simplified fourth-order contribution, coupling constants being treated as adjustable parameters. No comparison with theoretical predictions for this term was made. As a natural complement to that study, we have undertaken more accurate calculations of the anharmonic linewidth, based on an analytical expression of the crystal potential and on a formula which includes high-order contributions [9]. Such calculations are reported in the present work. This procedure was expected also to provide better estimates of the disorder term, by comparison with the experimental linewidth. We found that the relation between the disorder linewidth and the dispersion, due to disorder, of the mode frequency, is similar to the prediction of the ATA approximation for a crystal with no anharmonicity [10].

In the next section, we will described the model we used. Technical details on lattice dynamics calculations are given in section 3; experimental details have been given in the previous paper and will not be repeated here. In section 4 we will show and discuss our results. A brief conclusion follows.

2. THE MODEL

Our comparative study of Raman linewidths in BCB and DBB is based on the model described by Prasad and Von Smith [7], who applied it to the

Downloaded by [University of California, San Diego] at 11:43 21 August 2012

lowest Raman lattice model of BCB. The reader should refer to that paper for a detailed discussion of the theory. According to these authors, if the effect of disorder is treated in the CPA approximation [3], the global shape of the Raman line i is approximately lorentzian, with total width

$$\Gamma_i(T)=\Gamma_i^D+\Gamma_i^A(T) \tag{2.1}$$

where Γ_i^D is the term due to disorder and $\Gamma_i^A(T)$ is that due to anharmonicity.

This model is in good agreement with Raman spectra of BCB [7, 8], where all lattice bands show a lorentzian shape and internal bands are essentially lorentzian once the contribution of small side-bands is subtracted [8]. Other treatments that imply a non-lorentzian shape [10–13] appear less appropriate for the system under investigation, although the application of a model based on the ATA approach [10] has been considered for one of the internal bands [8].

The contribution to the lineshape due to disorder is a lorentzian under the following assumptions [7]: phonons are highly delocalised; orientational disorder does not mix different phonon branches of the ideal ordered lattice; only two-body, short range interactions are important; the investigated line is narrow. The authors use Raman spectra of mixed crystals of *p*-dihalobenzenes [14] to prove that the perturbative approach is correct even in the presence of complete head-tail disorder, and that the above assumptions are correct for the lowest frequency lattice band in BCB. We find that the same argument can be extended to all lattice bands and to internal phonon bands, with the possible exception of bands in the middle lattice frequency range, where a certain mixing of modes cannot be excluded.

In the Prasad-Von Smith model, the disorder contribution to the linewidth is considered to be temperature independent [7]. This amounts to assuming that cross-terms due to the combined effect of anharmonicity and disorder in the self-energy expansion can be disregarded. In fact, it can be shown that, in the temperature dependence of the linewidth, these terms are small with respect to the contribution of pure anharmonicity [15].

The anharmonic term $\Gamma_i^A(T)$ was originally modeled with one average 3-phonon process, coupling constants being treated as parameters [7]. The same approach was used in our previous paper [8], where an additional term representing 4-phonon scattering was considered. However, through this approach one cannot separate anharmonic constants from

Downloaded by [University of California, San Diego] at 11:43 21 August 2012

the scattering probability [16, 17]; also, the possible contribution of higher-order processes is ruled out from the beginning. In order to get a better description of the processes involved in anharmonic scattering, and to compare best-fit coefficients with theoretical values, in the present work we compute the anharmonic term from the double-vertex anharmonic self-energy series [9]

$$\Gamma_i^A(T) = \sum_{n=3}^{\infty} \Gamma_i^{(n)} = \sum_{n=3}^{\infty} C_i^{(n)} \rho^{(n-1)}(\omega_i, T) \tag{2.2}$$

where $C_i^{(n)}$ is an average squared coupling coefficient of order n and $\rho^{(n-1)}(\omega_i, T)$ is a weighted density of $(n-1)$-phonon states. State densities and coupling coefficients can be calculated with standard Lattice Dynamics techniques, if a realistic model for the disordered crystal is devised, as will be illustrated in the next section. Equation (2.2) is discussed in more detail in the Appendix.

The disorder contribution to the width of BCB bands, Γ_i^D, was treated in the preceding works [7, 8] as an adjustable parameter. To our knowledge, within this model no analytical formulation is available for the *a priori* calculation of such a contribution (although it can be evaluated with MD simulations [18]). Here we apply the same method, and also try to get some insight in the relationship between Γ_i^D and the nature of mode i. We found it useful to compare the dependence of Γ_i^D on i with that predicted in the ATA approximation [10] for a crystal with no anharmonicity and with a Gaussian distribution of site energy perturbations due to disorder. The result obtained for single-particle electronic excitations [10] is basically

$$\Gamma_i^D \propto D_i^2 \tag{2.3}$$

where D_i is the width of the gaussian distribution.

In our opinion, this result can be extended to phonon states with no critical change to the original treatment. However, we are interested in the concurrent effect of disorder and anharmonicity. If this is considered in the same model [10] it can be shown that, even with very strict assumptions (no interaction between phonon–phonon coupling and scattering due to disorder; no phonon dispersion), the self-energy term due to disorder depends on the term due to anharmonicity and cannot be decoupled from it; consequently, (2.3) is no more valid.

Bearing in mind all the approximations that we have illustrated, we represented the Prasad-Von Smith model with the following expression for

Downloaded by [University of California, San Diego] at 11:43 21 August 2012

the temperature-dependent linewidth of mode i of both DBB and BCB:

$$\Gamma_i(T) = \Gamma_i^0 + \sum_{n=3}^{\infty} C_i^{(n)} \rho^{(n-1)}(\omega_i, T), \tag{2.4}$$

where Γ_i^0 includes both the term due to orientational disorder (2.3) – if any – and all other temperature independent contributions (such as those due to impurities and instrumental resolution):

$$\Gamma_i^0 = \Gamma_i^D + \Gamma_i' \tag{2.5}$$

3. LATTICE DYNAMICS CALCULATIONS

In this section, we give some details on the calculation of the anharmonic linewidth – *equation (2.2)* – of the Raman active lattice modes and of some Raman active internal modes in DBB and BCB.

BCB and DBB crystallize in monoclinic lattice with two molecules per unit cell [19]. The former shows head-to-tail disorder due to two almost equivalent orientations of the molecules with respect to the halogen–halogen axis. Assuming a fully disordered structure, BCB belongs to the same space group (C_{2h}^5, $P2_1/a$) as the DBB crystal and follows the same selection rules [20, 21]; because of the inversion center symmetry, the phonons exhibit mutually exclusive Raman or IR activity. In evaluating the effect of disorder (see the next section) we also considered two hyphothetical ordered structures of BCB, (C_2^2, $P2_1$) and (C_s^2, Pa), both isomorphous with DBB, with the second molecule in the unit cell being related to the first one by either the screw axis or the slide plane.

No crystal structure at low temperature is reported in the literature. Since thermal expansion data are also not available, we made no attempt to arbitrarily extrapolate room temperature structure to low temperature. Thus, in our calculations we used cell parameters measured at room temperature [22, 23], with the molecular structure of DBB observed in the crystal by Bandoli *et al.* [19].

The only way of reproducing an orientationally disordered crystal structure in a lattice dynamics framework is to use an asymmetric unit made up of a large number N of unit cells, with a fraction of the molecules flipped according to some distribution law. The computational requirements of this kind of approach are very high, since the dimensions of the dynamical matrix grow up as N^2. We chose a different approach: since, according to

Downloaded by [University of California, San Diego] at 11:43 21 August 2012

investigators, the head-to-tail disorder of BCB is complete, we represented the crystal as made up of molecules with two fictitious atoms X in the place of either Cl or Br. The physical properties of X (mass, C-X bond length and the value of the potential function at each interatomic distance r) are exactly intermediate between those of bromine and those of chlorine.

The intermolecular potential parameters for lattice dynamics calculations were taken from a model set up for haloanthracene derivatives [24]. In this model the interactions are represented by a Buckingham atom–atom potential, as summarized in Table I. The introduction of an additional electrostatic term represented by point charges along carbon–halogen bonds did not improve the agreement between calculated and experimental harmonic frequencies at zero wave vector, as already reported in the literature [25], so we omitted this term in the final computations. Other potential parameter sets [25] gave comparable results.

Computed and experimental $\mathbf{k} = \mathbf{0}$ harmonic frequencies at room temperature for both crystals, the lattice modes symmetry species and their assignment to molecular motions are reported in Table II.

Using equations (A.5) and (A.8) of the Appendix we computed $\rho^{(n)}(\omega, T)$ for both crystals up to $n = 4$ at different temperatures in the range 1–300 K, sampling the Brillouin zone in about 700 **k** points.

A linear least-squares fit of experimental data points then yielded Γ_i^0 and $C_i^{(n)}$ $(n = 3, 4, 5)$ for each investigated band. The fit procedure was repeated with constraints whenever one or more parameters were not physically reasonable, for example whenever they had a negative value. In this case, one parameter was fixed to a quantity equal or close to the calculated value (see below) and the remaining parameters were refined. This procedure was possibly reiterated. When more than one set of parameters obtained in this

TABLE I Parameters of Buckingham atom–atom potential model [24]. $V(r) = \mathrm{A}e^{-\mathrm{B}r} - \mathrm{C}r^{-6}$

	Parameters		
ij	$A_{ij}(kJ)$	$B_{ij}(\text{Å}^{-1})$	$C_{ij}(kJ\text{Å}^6)$
C—C	48179.8	2.92	2818.5
C—H	6072.9	2.89	443.0
C—Cl	191193.7	3.16	6623.5
C—Br	70214.9	2.80	7053.7
H—H	765.5	2.86	69.6
H—Cl	24099.2	3.13	1041.1
H—Br	8850.3	2.76	1108.7
Cl—Cl	758720.1	3.04	16576.2
Br—Br	102327.9	2.67	17652.8

Downloaded by [University of California, San Diego] at 11:43 21 August 2012

TABLE II Experimental and calculated room temperature harmonic frequencies (cm^{-1}). R_x, R_y, R_z are the librations around the principal inertia axes x, y, z (in decreasing order of inertia moments)

DBB		*BCB*			
exp.[20]	*calc.*	*exp.*[20]	*calc.*	*symmetry*	*assignment*
20.0	15.8	22.0	17.7	B_g	R_x, R_y
37.5	24.6	42.5	31.1	A_g	R_x, R_y
39.0	29.6	41.5	36.6	B_g	R_x, R_y
40.5	29.9	47.0	41.4	A_g	R_x, R_y
93.0	90.1	94.0	95.3	A_g	R_z
96.0	92.1	98.0	98.8	B_g	R_z

way was considered acceptable, that set was chosen which gave either the lowest χ^2 or the best agreement with calculated values, or both.

Calculated approximate average coefficients, to be used as a check for best-fit coefficients, were calculated with equation (A.7) of the Appendix. High order potential derivatives were obtained from derivatives of dynamical matrix elements at random points of the Brillouin zone [9]. Since in our implementation of the lattice dynamics algorithm [26] internal modes are treated as intrinsically harmonic, check coefficients were calculated for lattice modes only.

4. RESULTS AND DISCUSSION

The temperature dependence of the width of Raman bands of DBB and BCB in the region of lattice modes and of two internal modes has been discussed in detail in the previous work [8], that we shall refer to as CTBS hereafter. Here we investigate the same data with the method described in the preceding sections.

We start by saying that, in a most general sense, our calculations confirm the picture given by the phenomenological analysis in CTBS, that is, all bandwidths are composed of a temperature-dependent part due to anharmonic relaxation processes of order three and higher, and of a constant term which is mainly due to disorder in BCB.

All data can be fitted very well to equation (2.4). The physical significance of the calculated curves is proved by the fact that, for all bands, best-fit coefficients $C_i^{(n)}$, reported in Table III, agree, in magnitude, with theoretical values obtained from approximate equation (A.7) (Tab. IV). From a qualitative point of view, we observe that for most modes the BCB coefficient is

TABLE III Best-fit anharmonic coupling coefficients and zero-order term for DBB and BCB bands. ω_i, Γ_i^0 in cm^{-1}; $C_i^{(n)}$ in cm^{-2}

	ω_i	Γ_i^0	$C_i^{(3)}$	$C_i^{(4)}$	$C_i^{(5)}$
DBB	20.0	0.07	$7.4 \cdot 10^{-2}$	$1.0 \cdot 10^{-4}$	$1.0 \cdot 10^{-7}$
BCB	22.0	0.49	$1.9 \cdot 10^{-1}$	$2.3 \cdot 10^{-4}$	$2.2 \cdot 10^{-6}$
DBB	37.5	0.04	$6.4 \cdot 10^{-2}$	$1.8 \cdot 10^{-4}$	$4.0 \cdot 10^{-6}$
BCB	42.5	3.64	$2.5 \cdot 10^{-1}$	$3.7 \cdot 10^{-4}$	$5.8 \cdot 10^{-6}$
DBB	39.0	0.13	$3.4 \cdot 10^{-2}$	$5.4 \cdot 10^{-4}$	$1.4 \cdot 10^{-6}$
BCB	41.5	4.40	$3.0 \cdot 10^{-2}$	$3.0 \cdot 10^{-4}$	$4.0 \cdot 10^{-6}$
DBB	40.5	0.05	$1.6 \cdot 10^{-1}$	$2.3 \cdot 10^{-4}$	$1.0 \cdot 10^{-6}$
BCB	47.0*	–	–	–	–
DBB	93.0	0.91	$4.2 \cdot 10^{-1}$	$1.8 \cdot 10^{-3}$	$6.3 \cdot 10^{-6}$
BCB	94.0	0.91	$7.4 \cdot 10^{-1}$	$1.3 \cdot 10^{-3}$	$3.0 \cdot 10^{-6}$
DBB	96.0	0.78	$4.2 \cdot 10^{-1}$	$1.0 \cdot 10^{-3}$	$5.0 \cdot 10^{-6}$
BCB	98.0	0.78	$6.5 \cdot 10^{-1}$	$1.6 \cdot 10^{-3}$	$3.3 \cdot 10^{-6}$
DBB	710.0	0.10	$2.6 \cdot 10^{-2}$	$3.0 \cdot 10^{-5}$	$1.0 \cdot 10^{-6}$
BCB	730.0	0.94	$4.0 \cdot 10^{-2}$	$2.0 \cdot 10^{-5}$	$3.0 \cdot 10^{-6}$
DBB	1070.0	0.55	$2.1 \cdot 10^{-2}$	$6.0 \cdot 10^{-5}$	$1.0 \cdot 10^{-6}$
BCB	1090.0	1.26	$4.5 \cdot 10^{-2}$	$3.0 \cdot 10^{-5}$	$2.0 \cdot 10^{-6}$

*Experimental data of this very weak band show so low a correlation that a fit is considered of no significance.

TABLE IV Calculated anharmonic coupling coefficients for DBB and BCB bands (ω_i in cm^{-1}; $C_i^{(n)}$ in cm^{-2})

	ω_i	$C_i^{(3)}$	$C_i^{(4)}$	$C_i^{(5)}$
DBB	20.0	$1.2 \cdot 10^{-1}$	$1.3 \cdot 10^{-3}$	$1.3 \cdot 10^{-6}$
BCB	22.0	$2.6 \cdot 10^{-1}$	$2.6 \cdot 10^{-3}$	$6.0 \cdot 10^{-6}$
DBB	37.5	$1.2 \cdot 10^{-1}$	$1.1 \cdot 10^{-3}$	$1.6 \cdot 10^{-6}$
BCB	42.5	$1.1 \cdot 10^{-1}$	$4.0 \cdot 10^{-3}$	$6.5 \cdot 10^{-6}$
DBB	39.0	$8.9 \cdot 10^{-2}$	$8.6 \cdot 10^{-4}$	$1.4 \cdot 10^{-6}$
BCB	41.5	$2.4 \cdot 10^{-1}$	$1.7 \cdot 10^{-3}$	$5.8 \cdot 10^{-6}$
DBB	40.5	$1.3 \cdot 10^{-1}$	$8.6 \cdot 10^{-4}$	$1.9 \cdot 10^{-6}$
BCB	47.0	–	–	–
DBB	93.0	$6.3 \cdot 10^{-1}$	$5.3 \cdot 10^{-2}$	$6.2 \cdot 10^{-5}$
BCB	94.0	$8.1 \cdot 10^{-1}$	$4.3 \cdot 10^{-2}$	$4.1 \cdot 10^{-5}$
DBB	96.0	$5.8 \cdot 10^{-1}$	$5.0 \cdot 10^{-2}$	$5.6 \cdot 10^{-5}$
BCB	98.0	$7.1 \cdot 10^{-1}$	$4.0 \cdot 10^{-2}$	$3.3 \cdot 10^{-5}$

bigger than the corresponding DBB one; and that the same relationship exists between calculated values, due to the fact that the BCB potential is slightly more repulsive, as shown also by the shift in the lattice frequencies. Quantitatively, $C_i^{(3)}$ and $C_i^{(5)}$ values compare well to their theoretical coun-

Downloaded by [University of California, San Diego] at 11:43 21 August 2012

Downloaded by [University of California, San Diego] at 11:43 21 August 2012

terparts – if one considers the approximations involved in the calculation of average coefficients. On the contrary, $C_i^{(4)}$ coefficients are about one order to magnitude smaller than predicted. Discrepancies between best-fit and theoretical values may be due to several causes. Obviously, since our potential was originally refined on harmonic properties only, one or more of its high-order terms may be incorrect; however, we found that different potentials do not give better agreement than the one we present here. Errors in theoretical values may be caused also by the fact that they were averaged over a special class of coefficients [9]. Finally, best-fit coefficients are probably underestimated since they compensate too high a value of calculated state densities in the lattice mode region (we recall that calculated phonon frequencies are smaller than experimental ones; this contraction of the phonon band raises the low-frequency tail of multiple state densities).

For some aspects, present results differ from our previous work. In CTBS, the width of the lowest B_g line in DBB was reproduced with a cubic process only, while the corresponding line in BCB required also a quartic contribution, which appears rather unrealistic. Our analysis has shown that a null quartic contribution to the DBB linewidth implies that the quartic coefficient in DBB be more than one order of magnitude smaller than that of BCB, which is not consistent with calculated values (Tab. IV); on the other side, a good fit to the data can be obtained with a $C^{(4)}$(DBB) of the same order of $C^{(4)}$(BCB) (Tab. III), that is, with a quartic contribution comparable to that in BCB. This is illustrated in Figure 1.

For the highest lattice DBB modes, a null constant and a bigger cubic contribution than in BCB was assumed in CTBS. Our fit of these linewidths indicates, instead, a smaller cubic coefficient than in BCB, in agreement with calculated values (Tab. IV), and the same Γ_0 in the two bands (Tab. III). As a consequence, the disorder contribution to the width of the BCB band is reduced (see below). The linewidth of the highest A_g mode is shown in Figure 2.

In the semiquantitative approach followed in CTBS, coupling constants contain both the average anharmonic coefficient and the relevant multiple state density (see the Appendix). This has a number of implications. For example, since the two-phonon difference state density is much smaller than the two-phonon sum state density, considering an equal coupling constant for 3-up and 3-down processes (Tab. II of CTBS) amounts to considering a much higher anharmonic coefficient for the former than for the latter; which is certainly less correct than assuming a single average coefficient for all processes of a given order, as we do in the present approach.

It has already been noted that anharmonic coupling increases with the mode frequency (Fig. 7 of CTBS). The present analysis shows that this is

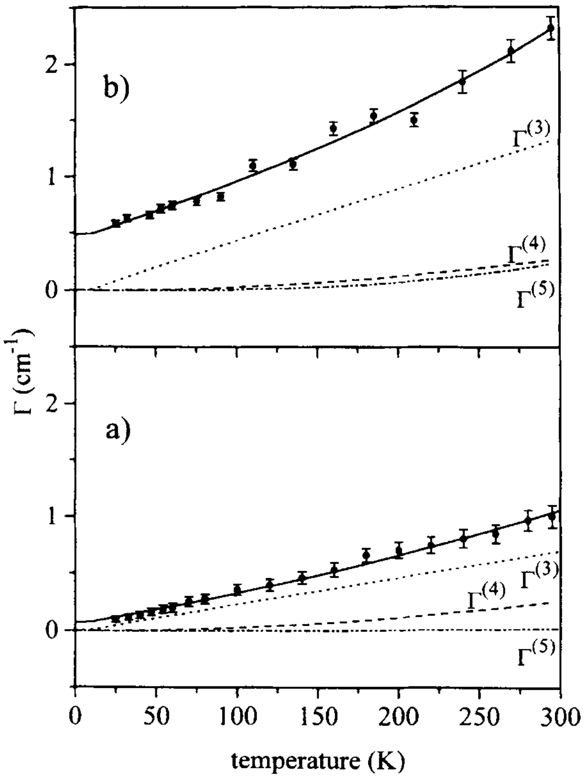

FIGURE 1 The temperature dependence of the lowest B_g lattice phonon linewidth in (a) DBB and (b) BCB. Points: experimental [8]; (—) $\Gamma_i(T)$, calculated with the parameters of Table III. The broken lines represent the contributions of processes of different order to $\Gamma_i(T)$.

due not only to the growing density of states, but also to increasing anharmonic coefficients (Tab. III), which roughly obey the relation $C_i^{(n)} \propto \omega_i$, as expected (see equations (A.4), (A.7) of the Appendix).

A detailed analysis of anharmonic relaxation is expected to yield more accurate best-fit values of Γ_i^0. As we already noted in the introduction, this quantity contains both the contribution of orientational disorder (in BCB) and the contribution of all other line broadening mechanisms that are independent of temperature (see eq. (2.3)). If we assume for the band i, Γ_i' is the same in DBB and BCB, the contribution of orientational disorder in BCB is simply given by the difference

$$\Gamma_i^D = \Gamma_i^0(\text{BCB}) - \Gamma_i^0(\text{DBB}). \tag{4.1}$$

Downloaded by [University of California, San Diego] at 11:43 21 August 2012

Downloaded by [University of California, San Diego] at 11:43 21 August 2012

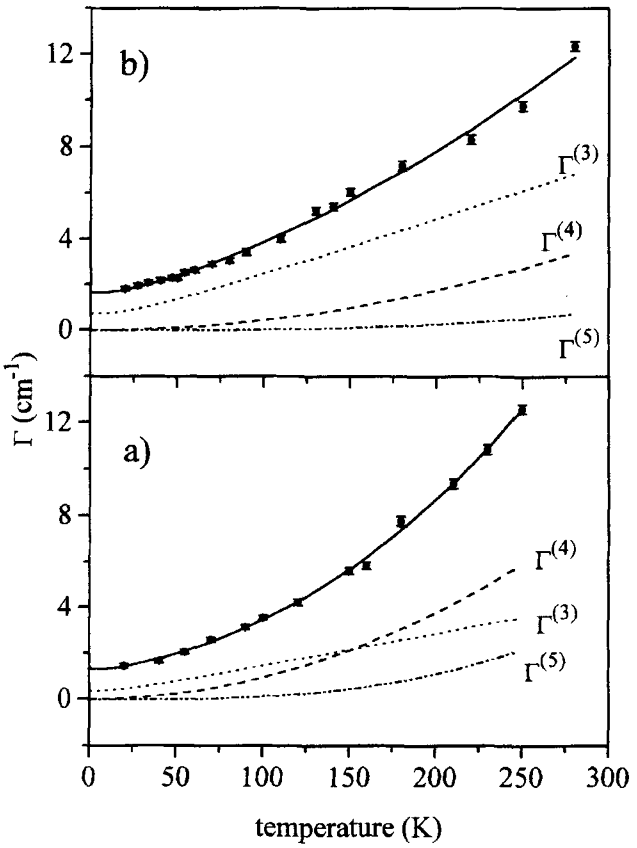

FIGURE 2 The temperature dependence of the highest A_g lattice phonon linewidth in (a) DBB and (b) BCB. Points: experimental [8]; (—) $\Gamma_i(T)$, calculated with the parameters of Table III. The broken lines represent the contributions of processes of different order to $\Gamma_i(T)$.

This difference is plotted in Figure 3. It shows a mamixum value for the modes around 40 cm^{-1}, while it is negligible, as expected, for the two librations around the *z* axis, that do not involve any motion of the halogen atoms. This result is probably more accurate than that reported in Table II of CTBS, where the disorder linewidth of the R_z modes is comparable to that of the lowest frequency mode.

We tried to established a relationship between Γ_i^D and the disorder "seen" by the mode *i*, as in (2.3). Unfortunately, there is no simple way of measuring or calculating the dispersion of perturbed levels, D_i, directly. A crude estimate of D_i may be given by the frequency shift of mode *i* between DBB

Downloaded by [University of California, San Diego] at 11:43 21 August 2012

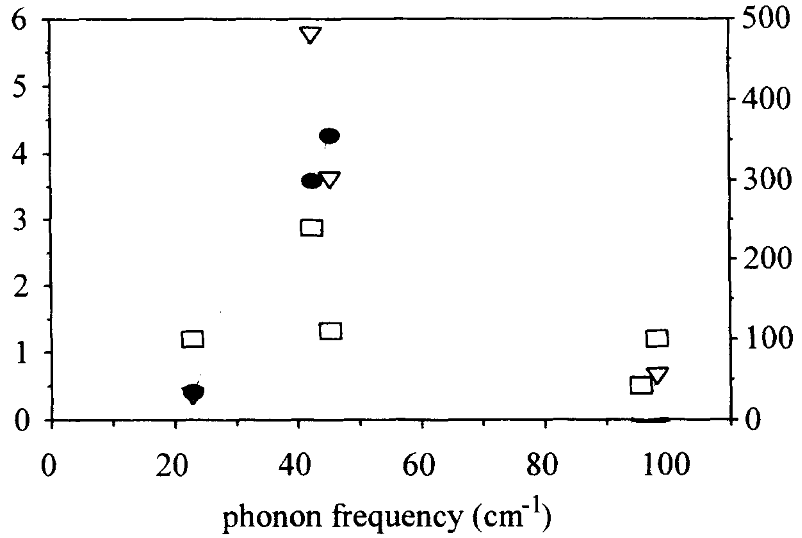

FIGURE 3 Contribution of orientational disorder to the width of lattice bands in BCB. Solid circles: Γ_i^D (cm^{-1}, eq. (4.1)); open triangles: square of frequency shift (cm^{-2}) between two ordered structures of BCB (scale on right-hand axis); open squares: square of frequency shift (cm^{-2}) between BCB and 1,4-dichlorobenzene (scale on right-hand axis).

and 1,4-dichlorobenzene. In fact, this shift measures the effect of substituting interactions involving Br with interactions involving Cl (although the change in the inertia moments and in the unit cell dimensions also contribute to this shift), the same effect that originates the average fluctuation D_i. The square of this shift is plotted in Figure 3. The obtain a more accurate measure of D_i, we calculated the frequency of mode *i* in two hypothetical ordered structures of BCB, C_2^2 and C_s^2, (see the previous section). The maximum frequency difference between one of the ordered structures and the fully disordered one was taken as an estimate of D_i and is reported (squared) in Figure 3. This figure shows that the relation (2.3) can be used as a guideline in the case of BCB. We consider this figure also as a confirmation of the validity of our model.

5. CONCLUSIONS

The calculations presented here globally confirm, with minor corrections, the results of the simplified analysis reported in a previous paper, thus indicating that the picture given there is physically meaningful. These re-

Downloaded by [University of California, San Diego] at 11:43 21 August 2012

sults are consistent with a perturbative model previously applied to the lowest lattice mode of BCB, according to which anharmonic coupling and orientational disorder give additive contributions to the optical phonon linewidth, the latter of which is approximately independent of temperature.

As for the anharmonic linewidth, this study, together with recent investigation on other crystals, shows that high order contributions can be calculated up to convergence of the self-energy, even at room temperature. Since in our approach only a special class of coupling schemes is considered, results are not expected to be accurate. Anharmonic coefficients that give the best agreement with experimental linewidths should therefore be regarded as effective values. In the present case, best-fit coefficients turn out to be comparable to values calculated from the intermolecular potential with an approximate method, with the exception of quartic coefficients. We point out that alternative approaches based on phenomenological expressions, as opposed to our approach, may be misleading, since they do not measure the values of the pure anharmonic coefficients. A few examples in this work where the present treatment leads to different conclusions from our previous paper have been illustrated.

Our anharmonic calculations have also enabled us to refine the values of the disorder contribution to the linewidth. The magnitude of this contribution is clearly dependent on the kind of motion involved in the decaying phonon, as already discussed on a qualitative basis in our previous work. We have found that this quantity is roughly proportional to the square of the energy dispersion of the mode due to disorder, a result that is similar to theoretical predictions for a harmonic crystal, and that suggests a simple method for the analysis of disorder contribution to linewidths in similar cases.

Acknowledgment

We wish to thank Professor V. Schettino for useful discussion and suggestions.

APPENDIX. ANHARMONIC LINEWIDTH SERIES

In the phonon–antiphonon picture, with frequencies ω_j taking both positive and negative values [9], the explicit form of the total linewidth of order n is

Downloaded by [University of California, San Diego] at 11:43 21 August 2012

$$\Gamma_i^{(n)} = \frac{2\pi}{\hbar(n-1)!}\left(\frac{\hbar}{2}\right)^n L^{2-n} \sum_{j_1 \dots j_{n-1}} \frac{|\Phi_{ij_1 \dots j_{n-1}}|^2}{|\omega_i \omega_{j_1} \dots \omega_{j_{n-1}}|} g(\omega_{j_1}) \dots g(\omega_{j_{n-1}}) \times$$

$$\times [\delta(\omega_i - (\omega_{j_1} + \cdots + \omega_{j_{n-1}})) - \delta(-\omega_i - (\omega_{j_1} + \cdots + \omega_{j_{n-1}}))] \times$$

$$\times \Delta(\mathbf{k}_i - (\mathbf{k}_{j_1} + \cdots + \mathbf{k}_{j_{n-1}})) \tag{A.1}$$

where

L is the number of cells in the lattice;

$L^{-n/2+1}\Phi_{ij_1 \cdots j_{n-1}}$ is the derivative of the crystal potential with respect to the n crystal normal coordinates labeled $i, j_1, \dots, j_{n-1}$;

$\delta(\omega)$ is the Dirac delta;

$\Delta(\mathbf{k})$ expresses the wavevector conservation [27] ($\mathbf{k}_i = \mathbf{0}$ for an optical band);

and we have defined

$$g(\omega_j) = \begin{cases} n(|\omega_j|, T) + 1 & \text{for } \omega_j > 0 \\ n(|\omega_j|, T) & \text{for } \omega_j < 0, \end{cases} \tag{A.2}$$

$$n(\omega_j, T) = [\exp(\hbar\omega_j / kT) - 1]^{-1}, \tag{A.3}$$

$C_i^{(n)}$ and $\rho^{(n-1)}(\omega_i, T)$ can be defined by comparison of (2.2) with (A.1). Considering that in the first approximation [9, 28]

$$\Phi_{ij_1 \dots j_{n-1}} \propto \omega_i \omega_{j_1} \dots \omega_{j_{n-1}}, \tag{A.4}$$

it appears most appropriate to define

$$\rho^{(n)}(\omega_i, T) = \hbar^{-1}[G^{(n)}(\omega_i, \mathbf{k}_i) - G^{(n)}(-\omega_i, \mathbf{k}_i)], \tag{A.5}$$

with

$$G^{(n)}(\omega, \mathbf{k}) = L^{2-n} \sum_{j_1 \dots j_n} \delta(\omega - (\omega_{j_1} + \cdots + \omega_{j_n})) \frac{|\omega_{j_1}|}{\langle \omega_{j_1} \rangle} \cdots \frac{|\omega_{j_n}|}{\langle \omega_{j_n} \rangle} g(\omega_{j_1}) \cdots g(\omega_{j_n}) \times$$

$$\times \Delta(\mathbf{k} - (\mathbf{k}_{j_1} + \cdots + \mathbf{k}_{j_n})) \tag{A.6}$$

Downloaded by [University of California, San Diego] at 11:43 21 August 2012

so that

$$C_i^{(n)} \approx \frac{2\pi}{(n-1)!}\left(\frac{\hbar}{2}\right)^n \frac{1}{|\omega_i|}\frac{1}{L^{n-1}} \sum_{j_1\dots j_{n-1}} |\Phi_{ij_1\dots j_{n-1}}|^2 \frac{\langle\omega_{j_1}\rangle}{\omega_{j_1}^2}\cdots\frac{\langle\omega_{j_{n-1}}\rangle}{\omega_{j_{n-1}}^2} \qquad \text{(A.7)}$$

which is exact in the limit (A.4) or, more generally, in the limit of no correlation between the sum arguments in $C_i^{(n)}$ and in $\rho^{(n-1)}$. In the last two equations we have introduced the quantity $\langle\omega_j\rangle$ which is the average value of the frequency of the j-th phonon branch. With these definitions $C_i^{(n)}$ and $\rho^{(n-1)}$ have the dimensions of E^2 and E^{-1}, respectively, where E is a molecular energy.

The advantage of the transformation of (A.1) into (2.2) is that many-phonon state densities $\rho^{(n)}$ can be calculated recursively from the one phonon density of states (which is usually known with good accuracy) using the relation [9]

$$G^{(n)}(\omega,\mathbf{k}) = \sum_{j_n}\frac{|\omega_{j_n}|}{\langle\omega_{j_n}\rangle} g(\omega_{j_n})\, G^{(n-1)}(\omega-\omega_{j_n}, \mathbf{k}-\mathbf{k}_{j_n}); \qquad \text{(A.8)}$$

(this calculation becomes trivial if the requirement of **k** conservation – the Δ factor in equation (A.6) – is relaxed, an approximation that has been shown to be the more accurate the higher n [29,30]). Note that a recursive algorithm of the type (A.8) cannot be applied to $\Gamma_i^{(n)}$ directly, due to the presence of the anharmonic coefficient.

Furthermore, $C_i^{(n)}$ can be evaluated with (A.7) by performing the sums over a small number of states, since $|\Phi_{ij_1\dots j_{n-1}}|$ is a slowly varying function of $\mathbf{k}_{j_1}\dots\mathbf{k}_{j_n}$ [9]. Average squared anharmonic coefficients can also be estimated with a linear fit of experimental linewidths to (2.2).

By using (2.2), anharmonic coefficients relative to different systems can be compared directly. Note that constants appearing in the widely-used approximate expressions of the type [1] $\Gamma_i^{(3)}(T) = B_i^{(3)} n(\langle\omega\rangle, T)$ are much less meaningful, since they include both anharmonic coefficients and state density.

We make one final remark. In (2.2) and in the following equations harmonic frequencies and anharmonic coefficients are assumed to be independent of temperature. This is no serious approximation in the case of lattice phonons. Thermal expansion of the crystal has a twofold effect on Γ_n: generally, anharmonic coefficients decrease with T, while the value of multiple state densities at ω_i increases with T due to the contraction of the phonon band. Thus, in general, the net effect on (2.2) will be negligible. Sample calculations [31] have confirmed this prediction.

Downloaded by [University of California, San Diego] at 11:43 21 August 2012

References

[1] S. Califano and V. Schettino, *Int. Rev. Phys. Chem.*, **7**, 19 (1988).
[2] A. A. Maradudin, E. W. Montroll, G. H. Weiss and I. P. Ipatova, "Theory of Lattice Dynamics in the Harmonic Approximation", *Solid State Physics* Vol. **3**, edited by F. Seitz, D. Turnbull, H. Ehrenreich (Academic, New York, 1971).
[3] R. J. Elliott, in "Lattice Dynamics and Intermolecular Forces" (Academic, New York, 1975), 342.
[4] A. Klug, *Nature*, **160**, 570 (1947).
[5] B. Wincke, A. Hadni and X. Gerbaux, *J. Phys.*, **31**, 893 (1970).
[6] A. Y. Korets, V. P. Fedorov and A. I. Shtain, *Opt. Spectrosc.*, **37**, 562 (1974).
[7] P. N. Prasad and R. Von Smith, *J. Chem. Phys.*, **71**, 4646 (1979).
[8] B. Caldarone, C. Taiti, R. Bini and V. Schettino, *J. Chem. Phys.*, **102**, 6653 (1995).
[9] P. Procacci, G. F. Signorini and R. G. Della Valle, *Phys. Rev. B*, **47**, 11124 (1993).
[10] J. Klafter and J. Jortner, *J. Chem. Phys.*, **68**, 1513 (1978).
[11] I. I. Abram and R. M. Hochstrasser, *J. Chem. Phys.*, **72**, 3617 (1980).
[12] S. Velsko and R. M. Hochstrasser, *J. Chem. Phys.*, **82**, 2180 (1985).
[13] E. L. Chronister and R. A. Crowell, *J. Phys. Chem.*, **95**, 2420 (1991).
[14] J. C. Bellows and P. N. Prasad, *J. Chem. Phys.*, **66**, 625 (1977).
[15] A. A. Maradudin and S. Califano, *Phys. Rev. B*, **48**, 12628 (1993).
[16] C. Taiti, P. Foggi, G. F. Signorini and V. Schettino, *Chem. Phys. Letters*, **212**, 283 (1993).
[17] G. F. Signorini, M. Becucci and E. Castellucci, *Chem. Phys.*, **187**, 263 (1994).
[18] G. Cardini, G. F. Signorini, P. R. Salvi and R. Righini, *Chem. Phys. Letters*, **142**, 570 (1987).
[19] G. Bandoli, D. A. Clemente, U. Croatto and C. Panattoni, *Gazz. Chim. Ital.*, **101**, 99 (1971).
[20] N. Le Calvé, S. Parent, B. Pasquier and F. Romain, *J. Raman Spec.*, **2**, 431 (1974).
[21] B. Pasquier, D. Bougeard, N. Le Calvé and R. Romain, *Mol. Cryst. Liq. Cryst.*, **32**, 17 (1976).
[22] A. Maiga, Nguyen-ba-Chanh, Y. Haalt and M. A. Cuevas-Diarte, *J. Appl. Cryst.*, **17**, 211 (1984).
[23] M. Labrador, E. Tauler, Y. Hagelt, T. Calvet, M. A. Cuevas-Diarte and E. Estop, *J. Appl. Cryst.*, **18**, 542 (1985).
[24] R. G. Della Valle and A. Brillante, *J. Chem. Phys.*, **100**, 7640 (1994).
[25] H. Bonadeo, E. D'Alessio, E. Holac and E. Burgos, *J. Chem. Phys.*, **68**, 4714 (1978).
[26] S. Califano, V. Schettino and N. Neto, "Lattice Dynamics in Molecular Crystals" in Lecture Notes Chem., **26** (Springer-Verlag, Berlin 1981).
[27] M. Born and K. Huang, "Dynamical Theory of Crystal Lattices", Oxford University Press (1954).
[28] R. E. Peierls, "Quantum theory of solids", Oxford University Press, New York (1955).
[29] R. G. Della Valle and G. Cardini, *Phys. Rev. Lett.*, **59**, 2196 (1987).
[30] R. G. Della Valle, G. F. Signorini and P. Procacci, *Phys. Rev. B* (1997).
[31] G. F. Signorini and L. Poletti, unpublished results (1993).